SLAC – PUB – 3368
June 1984
T/E/AS

# NONPERTURBATIVE EFFECTS IN EQUILIBRIUM FINITE TEMPERATURE SCALAR FIELD THEORY*

HIDEAKI AOYAMA AND HELEN R. QUINN

*Stanford Linear Accelerator Center*
*Stanford University, Stanford, California, 94305*

## ABSTRACT

The effects of nonperturbative configurations at finite temperature are investigated for a real scalar field theory that exhibits a spontaneous symmetry breaking at zero temperature. In 1+1 dimensions we find a zero temperature phase transition due to kink-antikink pairs. In 3+1 dimensions we calculate the contribution of bubbles that have an interior region of different vacuum in the equilibrium finite temperature theory. We find that the energy cost of bubble surfaces makes their effects negligible at temperature below the perturbatively calculated phase transition temperature. We discuss the interpretation of these results.

Submitted to *Physical Review D*

* Work supported by the Department of Energy, contract DE – AC03 – 76SF00515

# 1. Introduction

We have investigated the nonperturbative corrections to finite temperature field theory in a real scalar field theory that exhibits spontaneously broken symmetry at zero temperature. We calculate the effect of having regions of spacetime in which the scalar field expectation value has the opposite sign from that of the zero temperature vacuum, which is not counted in the usual perturbative, or self consistent treatment of the finite temperature field theories.

In a two dimensional theory these effects come from kinks and antikinks. In the equilibrium, the kinks and the antikinks can exist with certain probability. If we start from a vacuum $\langle\phi\rangle = v$ at zero temperature and raise the temperature slowly, the kinks and antikinks are created in pairs so that they conserve the total topological number. The regions between the kink and antikink are in the opposite vacuum $\langle\phi\rangle = -v$. By calculating the rate of these topological excitations, we derive the average thermal expectation value of the field operator. The effects are dramatic—they lower the symmetry-restoration phase transition to zero temperature. However this is a peculiar result which depends on the fact that the energy of separated kink and antikink configurations are independent of their separation.

In higher dimensional theories, the regions of the oposite vacuum are typically bubble-like, surrounded by the domain walls. We present the method of calculating the effects of a dilute gas of thin-walled bubbles in the framework of the imaginary-time path-integral formalism of finite temperature field theories. We show that, if the order $\lambda T^2$ corrections are ignored, this calculation indicates that there is an Ising-like phase transition at a temperature of order $\mu/\lambda$. However when the order $\lambda T^2$ shifts of effective mass and classical fields are self-consistently included they yield a phase transition at a temperature of order $\mu/\sqrt{\lambda}$ (which for weak coupling is a much lower temperature). Up to this temperature, bubble effects play a negligible role, because of the large surface energy cost of bubbles.

The outline of this paper is as follows:

In section 2 we present an intuitive picture of the effects included in the usual finite temperature field theory formalism and some comments on the region of validity of this formalism.

Section 3 presents our results for a two dimensional theory, first a heuristic argument and then a complete path integral treatment of the effects of kinks in dilute gas approximation. In this section, we also investigate the case where there is a energy density difference between two vacua, which is a good illustration of the techniques necessary to investigate higher dimensional theory. (Such a theory of course has no symmetry, and no phase transition, but one can still investigate corrections to the finite temperature perturbative theory, which can be large for sufficiently small energy density difference.)

In section 4 we present the dilute gas bubble calculation of bubble effects in 4 dimension.

Section 5 discusses the physical interpretation of our results and makes some comments on their implications for the more interesting case of gauge field theories.

## 2. Review of Perturbative Analysis

We will base our calculations on evaluations of non-perturbative effects in the Euclidean path integral calculated with periodicity $\beta = 1/T$ in the time direction.[1] However there are also real space-time techniques for calculating correlation functions at finite temperature which give results equivalent to the Euclidean methods.[2] For the purpose of this section, which is to provide an intuitive understanding of our calculations, we find it convenient to use a language which corresponds more nearly to the real space calculations, namely the language of Hamiltonian quantum mechanics. In this language we may call a field configuration at fixed time a state of the system and we may choose to span the states of the system with any complete basis set. In this section we mainly discuss the four dimensional case. The 1+1 dimensional case is mentioned later.

Consider the Lagrangian for a (positive mass squared) real scalar field,

$$\mathcal{L} = \frac{1}{2}(\partial\phi)^2 + \frac{m^2}{2}\phi^2 + \frac{\lambda}{4}\phi^4 \,. \tag{2.1}$$

The mass $m$ and coupling constant $\lambda$ are defined by zero-temperature renormalization prescriptions. We chose them to be the physical mass and the on-shell four-point function of the theory. A convenient basis in which to discuss this theory, for small $\lambda$, is the set of all free field momentum eigenstates of mass $m$. In terms of the fields $\phi_k$ and their canonically conjugate momenta $\pi_k$ the Lagrangian (2.1) leads to a Hamiltonian

$$H = \int \frac{d^3k}{(2\pi)^3}\left(\pi_k^2 + (k^2+m^2)\phi_k^2\right)$$
$$+ \frac{\lambda}{4}\int\frac{d^3k_1}{(2\pi)^3}\int\frac{d^3k_2}{(2\pi)^3}\int\frac{d^3k_3}{(2\pi)^3}\int d^3k_4\,\delta^3(k_1+k_2+k_3+k_4)\phi_{k_1}\phi_{k_2}\phi_{k_3}\phi_{k_4} \tag{2.2}$$

To zeroth order in the coupling constant $\lambda$ the harmonic oscillator modes have energies $E_k^0 = (k^2+m^2)^{1/2}$.

The finite temperature formalism corresponds to evaluating

$$\langle \mathcal{O} \rangle_\beta = \frac{\sum_n \langle n | \mathcal{O}\, e^{-\beta H} | n \rangle}{\sum_n \langle n |\, e^{-\beta H} | n \rangle} \tag{2.3}$$

where the states $|n\rangle$ form a complete set of the theory. A loop expansion of the Schwinger-Dyson diagrams can be made at any temperature. One finds that at high temperature, loops with multiple propagators can contribute terms of order $\mathcal{O}(\lambda T/m)$ per loop, while the diagram in which a single propagator loop closes itself (see Fig.1) contributes a mass correction, $\frac{1}{4}\lambda T^2$. At high enough temperature, this quantity is not small even for weak coupling, so a straightforward loop expansion breaks down. However, since the graph with a single propagator loop appears only as a mass insertion, it can be included to all orders by evaluating all graphs with the mass set to

$$m_{\rm eff}^2(T) \equiv m^2 + \frac{1}{4}\lambda T^2 \quad . \tag{2.4}$$

Multi-propagator loops then are counted explicitly, they contribute at most $\mathcal{O}(\lambda T/m_{\rm eff}(T))$ per loop at high temperature. We will call this procedure the modified loop expansion. The leading high temperature correction to $m_{\rm eff}^2(T)$ are unchanged from the usual one-loop calculation because the $\mathcal{O}(T^2)$ contribution of the single-propagator-loop graph is independent of the mass of the propagator. However now higher loop corrections are seen to be controlled, since $\mathcal{O}(\lambda T/m_{\rm eff}(T))$ is of order $\sqrt{\lambda}$ for very high $T$. At very low temperature, difference between the results of modified loop expansion and the loop expansion are negligible.

Physically the difference between the loop expansion and the modified loop expansion can be understood in this way. In the loop expansion we begin with a thermal distribution of states populated with a weight $\exp(-\beta E_k^0)$ and the effect of interactions between the populated modes as well as between the externally

produced particles and these modes are calculated order by order in perturbation theory. In the modified loop expansion we recognize that the interaction changes the energy cost of a mode and hence we populate the modes with a weight $\exp(-\beta E_k^T)$, thus including the dominant high temperature correction to all orders. However in both cases the treatment is based on free field theory modes and their interactions.

Let us now consider a theory where spontaneous symmetry breaking occurs in the zero-temperature theory and see how the usual finite temperature phase transition arises in this language. Let

$$\mathcal{L} = \frac{1}{2}(\partial\phi)^2 - \frac{1}{2}\mu^2\phi^2 + \frac{\lambda}{4}\phi^4 \,. \tag{2.5}$$

Now in addition to the finite $k$ quantum modes we must allow for a non-trivial $k = 0$ classical field. In the positive $m^2$ case such a field will always be found to have the solution $\langle\phi\rangle = 0$ even at finite temperature. With the Lagrangian (2.5), at zero temperature, the negative $\mu^2$ term leads to

$$\langle\phi\rangle_{T=0} = \pm\frac{\mu}{\sqrt{\lambda}} \equiv \pm v \; ; \quad m^2 = 2\lambda\, v^2 = 2\mu^2 \,, \tag{2.6}$$

as the possible consistent solutions of the Schwinger-Dyson equations. These solutions are usually described as the turning points of some $V_{\rm eff}(\phi_0)$ with $\partial^2 V_{\rm eff}/\partial\phi^2 > 0$. (There is a problem in defining $V_{\rm eff}(\phi_0)$ such that $\partial^2 V_{\rm eff}/\partial\phi^2$ is negative. This problem is irrelevant to the physical discussion here, which is why we prefer to use the language of solutions of the Schwinger-Dyson equations, which does not require a $V_{\rm eff}(\phi_0)$ to be defined.) Again we choose our renormalization prescriptions so that $m$ and $\lambda$ are the physical zero temperature mass and on-shell four-point function, and we select $\langle\phi\rangle_{T=0} = +v$ as the zero temperature vacuum. When we examine the finite temperature theory we also include the effect of the thermal population of the quantum modes on this classical field via the modified loop expansion. The effect of occupying the finite

$k$-modes with a thermal distribution is to shift the consistent value of the classical field towards zero. Thus the usual finite temperature phase transition is seen to be due entirely to including the thermal fluctuations about the constant classical field vacuum state. The calculation predicts a second order phase transition at $T = 2\mu/\sqrt{\lambda}(\equiv T_c)$ where $m_{\rm eff}(T_c) = 0$. However clearly $\lambda T/m_{\rm eff}$ is not small in this region, so that further care is needed to treat this region reliably, the loop expansion (modified or not) is not sufficient very near the phase transition.

The solutions of the Schwinger-Dyson equation for $\langle\phi\rangle_T$ are shown in Fig 2. Case (a) is the model given by the Lagrangian (2.5). When a term of the form $\epsilon\phi^3$ is added (when there is no symmetry and no phase transition), we obtain case (b). The dotted lines in the figures indicate the regions where the calculation is unreliable because $\lambda T/m_{\rm eff}$ is not small inside these regions.

In 1+1 dimensions the situation is not so simple at finite temperature. One finds every loop (including the single propagator loop) can give at most $\mathcal{O}(\lambda T/m)$ corrections and there is no justification for summing mass insertion loops differently from any other loop correction. The loop expansion is satisfactory only at low enough temperatures that $T/m$ is small. Once again the expansion breaks down at temperatures below those where it predicts a phase transition. But in this case, it does not recover at high temperature as it does in the 3+1 dimensional case.

As we have seen above, in models defined by the Lagrangian (2.5) the loop calculations give some reasonable treatment of certain thermal excitations. However there are other possible low-lying states which may be very poorly treated by this perturbative evaluation. These are states in which regions of space $R$ have $\langle\phi(x)\rangle = -v(T)$ for $x \in R$ and $\langle\phi(x)\rangle = v(T)$ elsewhere. In 1+1 dimensional spacetime, the regions $R$ are regions between kinks and antikinks. In the higher dimensional spacetime, these regions are bubble like. These states have some surface energy cost due to the interfaces between the regions with different signs of $\phi(x)$. Of course, since the free field momentum eigenstates form

a complete set of states one can in fact span the bubble states by a complicated superposition of momentum eigenstates, but the perturbative calculation does not populate these states with the correct probability at finite temperature, and hence may grossly underestimate their contribution.

This paper is devoted to a study of the effect of such configurations at finite temperature. We calculate how the usual perturbative picture is corrected when these modes, and fluctuations about them, are included explicitly in the finite temperature calculation. We find the effect is dramatic in $1+1$ dimensions — the phase transition occurs at zero temperature. However this is truly a peculiarity of $1+1$ dimensions due to the fact that there is no additional energy cost for configurations in which kinks and antikinks are widely separated. In higher dimensions bubbles have an energy proportional to their surface area (in thin-walled approximation). In this case we find that the corrections to the usual perturbative treatment are very small.

## 3. 1+1 Dimensional Case

In this section, we discuss the distribution of states reached by raising the temperature, starting from the vacuum state $\langle\phi\rangle = v$. The system is described by the Lagrangian (2.6) in 1+1 dimensions.

The spectrum of this theory consists of the perturbative modes (real scalar particles) and nonperturbative modes. The nonperturbative modes are kinks and antikinks that are given by the following solutions of the classical field equations,

$$\phi_s(x - X) = \pm v \tanh \frac{\mu(x - X)}{\sqrt{2}} \quad . \tag{3.1}$$

(We call the solution with the positive sign the kink and the other the antikink.) These solutions have energy (mass),

$$\rho = \frac{2\sqrt{2}\,\mu^3}{3\lambda} \quad . \tag{3.2}$$

The fact that coupling constant $\lambda$ appears in the denominator illustrates the nonperturbative nature of this mode. The interaction between these kinks is exponentially small for distances larger than their thickness, $\frac{1}{\mu}$. For our purposes this interaction is negligible, the kinks are essentially free. At finite temperature, both the perturbative modes and the nonperturbative modes are excited. As we raise the temperature, the kinks and the antikinks are created in pairs with the kink to the left of the antikink. (The spatial boundary condition is always $\phi = v$ at $x \to \pm\infty$ in our calculation.)

We begin with a semiclassical discussion which indicates the major features of the effects due to the kinks. We will then present a more complete treatment of the finite temperature path-integral calculation of these effects.

## 3.1 Quantum Mechanics of Kinks

Let us confine the kinks (and antikinks) in a box of length $L$. The normalized wavefunctions for a kink at $X$ and an antikink at $Y$ are given as follows,

$$\psi_{(m,n)}(X,Y) = (\sin(k_{m+n}X)\sin(k_nY) - \sin(k_nX)\sin(k_{m+n}Y))\Theta(Y-X) \quad , \tag{3.3}$$

where $k_n \equiv \pi n/L$. The quantum numbers are $m = 1,2,3,....$ and $n = 1,2,3,.....$ These wavefunctions are chosen to satisfy the boundary conditions,

$$\psi(0,Y) = \psi(X,X) = \psi(X,L) = 0 \quad . \tag{3.4}$$

In between the kink and the antikink, the scalar field $\phi$ takes the value $-v$. Thus once the probability $P(Z)$ of the point $Z$ being in between the pair is given, the expectation value of the field is given by $\langle\phi(Z)\rangle = v\,(1-2\,P(Z))$. In the $(m,n)$ state given by (3.3), this probability is as follows,

$$\begin{aligned} P_1^{(m,n)}(Z) = \frac{1}{2}\Big[1 - \Big(\frac{2Z}{L} - 1 - \frac{\sin(2k_{m+n}Z)}{2k_{m+n}}\Big)\Big(\frac{2Z}{L} - 1 - \frac{\sin(2k_mZ)}{2k_m}\Big) \\ + \Big(\frac{\sin(k_mZ)}{k_m} - \frac{\sin(k_{2n+m}Z)}{k_{2n+m}}\Big)^2\Big] \quad . \end{aligned} \tag{3.5}$$

The average value of this probability is of physical interest. It is,

$$\overline{P}_1^{(m,n)} = \frac{1}{L}\int_0^L dZ\, P_1^{(m,n)}(Z) = \frac{1}{3} + \frac{1}{L^2}\left(\frac{1}{k_m^2} + \frac{1}{k_{2n+m}^2} - \frac{1}{2k_{n+m}^2} - \frac{1}{2k_n^2}\right) \quad . \tag{3.6}$$

One can obtain this same result for the leading term in the $L \to \infty$ limit by approximating $\psi_{(m,n)}$ by $\psi_{(m,n)} \propto \Theta(Y-X)$, that is, by neglecting to impose the boundary conditions (3.4) .

In the multi-pair sectors, we can estimate the large volume limit of $P$'s using this same constant wavefunction. The wavefunction of $N$-pairs is assumed to be,

$$|\psi_N|^2 = \frac{(2N)!}{L^{2N}} \Theta(X_1 - Y_1)\Theta(Y_1 - X_2)....\Theta(Y_{N-1} - X_N)\Theta(X_N - Y_N) \quad . \tag{3.7}$$

The corresponding probabilities are given by,

$$P_N(Z) = \frac{1}{2}\left[1 - \left(\frac{2Z}{L} - 1\right)^{2N}\right] \quad , \tag{3.8}$$

$$\overline{P}_N = \frac{N}{2N+1} \quad . \tag{3.9}$$

Heuristically, the statistical weight of one kink is,

$$\Delta = \sum_n e^{-\beta\sqrt{k_n^2+\rho^2}} \overset{L\to\infty}{\longrightarrow} L\int \frac{dk}{2\pi} e^{-\beta\sqrt{k^2+\rho^2}} \quad . \tag{3.10}$$

Therefore, ignoring kink interactions, we can sum the multi-pair contributions to obtain

$$\begin{aligned} \overline{P} &= \frac{\sum_{N=0}^{\infty} \overline{P}_N \frac{1}{(2N)!}\Delta^{2N}}{\sum_{N=0}^{\infty} \frac{1}{(2N)!}\Delta^{2N}} \quad , \\ &= \frac{1}{2}\left(1 - \frac{\tanh\Delta}{\Delta}\right) \quad . \end{aligned} \tag{3.11}$$

Since $\Delta$ diverges like $L e^{-\beta\rho}$ in the infinite volume limit, we find

$$\overline{P} \overset{L\to\infty}{\longrightarrow} \frac{1}{2} \quad . \tag{3.12}$$

Therefore, we obtain

$$\langle\phi\rangle_T \equiv \langle\frac{1}{L}\int dx\phi(x)\rangle_T = v(1 - 2\overline{P}) \overset{L\to\infty}{\longrightarrow} 0 \quad , \tag{3.13}$$

for any $T \neq 0$. Thus we see that the phase transition takes place at zero temperature. The crucial feature of this argument is that there is no suppression

of the states where the kink and antikink are widely separated because there is no attraction between them. Note that we have shown here that the disordered phase (3.13) is realized, but for any x $\langle|\phi(x)|\rangle$ is of order $v$ (near $T = 0$).

## 3.2 Quantum Field Theory of Kinks

We now derive the result in the previous subsection more precisely, treating the kinks and fluctuations about them according to the standard Euclidean path-integral formalism of finite temperature field theory.[3] The generating functional of the theory is given by,

$$Z(T) = \int [d\phi] \exp\Big(-\int_{-\frac{\beta}{2}}^{\frac{\beta}{2}} d\tau \int dx \mathcal{L}[\phi]\Big) \quad . \tag{3.14}$$

This functional integral is restricted to the periodic functions of $\phi$,

$$\begin{aligned} \phi\left(-\frac{\beta}{2}, x\right) &= \phi\left(\frac{\beta}{2}, x\right) \quad , \\ \frac{\partial}{\partial\tau}\phi\left(-\frac{\beta}{2}, x\right) &= \frac{\partial}{\partial\tau}\phi\left(\frac{\beta}{2}, x\right) \quad . \end{aligned} \tag{3.15}$$

We want to calculate the contribution to this path-integral from kinks, antikinks, and the fluctuations about them. We will use the usual background field collective coordinate formalism to discuss a dilute gas of kinks and antikinks. For a single kink whose center follows the path $X(\tau)$, we can take the background field to be,

$$\phi_{bg}(\tau, x) = \phi_s\left(\frac{x - X(\tau)}{\sqrt{1 + \dot{X}(\tau)^2}}\right) \quad . \tag{3.16}$$

For this configuration, the boundary conditions (3.15) translates into the follow-

ing,

$$X\left(-\frac{\beta}{2}\right) = X\left(\frac{\beta}{2}\right), \quad \dot{X}\left(-\frac{\beta}{2}\right) = \dot{X}\left(\frac{\beta}{2}\right) \quad . \tag{3.17}$$

The action corresponding to this background field is,

$$\mathcal{A}_{kink} = \int_{-\frac{\beta}{2}}^{\frac{\beta}{2}} d\tau\, \rho\sqrt{1+\dot{X}(\tau)^2} \quad . \tag{3.18}$$

where we have dropped terms proportional to $\ddot{X}(\tau)$, hence assuming that acceleration is small. This action is minimized by solving the classical equation of motion for $X(\tau)$. The only solutions which satisfy the periodic boundary conditions (3.15), are the form $X(\tau) = constant$, which describes a *static* kink (or an antikink). Clearly the assumption of small acceleration is consistent with this solution.

According to the standard treatment of the solitons, the one-loop expression of one pair sector of the generating functional $Z(T)$ (3.14) is expressed as follows,

$$\Delta_1 \equiv \frac{Z_1(T)}{Z_0(T)} = e^{-2\beta\rho}\int J_X dX\, J_Y dY\, [d\phi_f]' e^{-\frac{1}{2}D[\phi_{pair}]\phi_f^2} \quad . \tag{3.19}$$

where $X$ and $Y$ denote the spatial positions of the (static) kink and the antikink. This expression is obtained by changing two of the path-integral variables, namely the (static) translation modes, into the collective coordinates, $X$ and $Y$. The prime on $d\phi_f$ means that among the fluctuations around the kinks these zero modes are excluded from the integration. The Jacobian factors, $J_X$ and $J_Y$ are given by

$$J_X = \frac{1}{\sqrt{2\pi}}\sqrt{\int dx d\tau \left(\frac{\partial\phi_{pair}(x,\tau,X,Y)}{\partial X}\right)^2} = \sqrt{\frac{\beta\rho}{4\pi}} \quad , \tag{3.20}$$

and similarly for $J_Y$. (The factor $1/\sqrt{2\pi}$ arises because we have one less Gaussian integral.[4] ) The normalization factor $Z_0(T)$ is the path-integral without any

kinks. We evaluate (3.19) as follows,

$$\Delta_1 = e^{-2\beta\rho} \int J_X dX\, J_Y dY \sqrt{\frac{det D(\phi_{bg} = v)}{det' D(\phi_{pair})}} \quad . \tag{3.21}$$

In the approximation that kink-antikink interactions can be ignored, the ratio of the determinants needed for evaluating (3.21) is the square of the single kink contribution, which is given in appendix A. We obtain,

$$\Delta_1 = e^{-2\beta(\rho+\Delta\rho)} \frac{\beta\rho}{4\pi} \frac{1}{\beta^2} F_T \int_0^L dY \int_0^Y dX \quad , \tag{3.22}$$

where $F_T$ represents the finite temperature effects that comes from the determinant. The $\Delta\rho$ in the exponent represents the zero temperature mass correction. Note that the collective coordinate integral has a trivial integrand 1. This is because we ignored the effect of boundaries, $X = 0$, $X = Y$ and $Y = L$ (we only did the Gaussian integrations of the fluctuations). These boundary conditions are irrelevant in the large volume limit as we saw in (3.6) . The expression (3.22) corresponds to the constant wavefunction of the form of (3.7) . Hence we see that the result of the heuristic argument of the probabilities $P$'s are unchanged except that the quantity $\Delta_1$ replaces the naively estimated $\Delta$ in eq. (3.11)

Actually, the fluctuations around the kinks have nontrivial contributions to the thermal expectation value $\langle\phi\rangle$, which was not included in the heuristic argument. This is the distortion of the kinks due to the presence of the fluctuations. Far from the kinks, these effects yield $v(T)$, the perturbative value of $\langle\phi\rangle$. Because of this, the thermal expectation value of the $\phi$ field is given by

$$\langle\phi\rangle_T = v(T)[1 - 2\overline{P}(\rho(T))] \quad . \tag{3.23}$$

However since the volume divergence of $\Delta_1$ leads to *the zero temperature phase transition*, the temperature dependence of $v$ and $\rho$ is unimportant in this case.[5]

The consistency of the free-kink approximation can be confirmed by calculating the average distance $\overline{D}$ between kinks. By using the expression (3.9) and doing the similar calculation to (3.11), we obtain the following large $L$ limit,

$$\overline{D} = \frac{L}{\sqrt{\Delta}} = e^{\beta\rho}\sqrt{\frac{4\pi\beta}{\rho F_T}}, \tag{3.24}$$

For low temperature $T \ll \rho$ we are interested in, the exponent gives a large factor. Thus $\overline{D} \gg 1/\mu$ is satisfied. Hence it was consistent to assume that the kinks are separated by large distances and we can neglect the overlap between them.

### 3.3 Non-degenerate Case

We now turn to the case of the theory with a small $\phi^3$ term in the potential. This theory has no symmetry and no phase transition at finite temperature. However we include here a discussion of the corrections to the finite temperature perturbative treatment of this theory, because it is the simplest example which exhibits features similar to those of the symmetric theory in higher dimension. This enables us to discuss in the simpler context techniques which we find necessary to use in the higher dimensional symmetric theory.

Consider the Lagrangian,

$$\mathcal{L} = \frac{1}{2}(\partial\phi)^2 - \frac{1}{2}\mu^2\phi^2 - \frac{\epsilon}{3}\phi^3 + \frac{\lambda}{4}\phi^4 \quad . \tag{3.25}$$

We can choose $\epsilon$ to be positive without loss of the generality. We are interested in the case $\epsilon \ll \lambda$. For this theory the effective potential at $T = 0$ has two minima; a global minimum at $\langle\phi\rangle = v + O(\epsilon)$ and a local minimum at $\langle\phi\rangle = -v + O(\epsilon)$. At the local minimum the energy density is higher by an amount,

$$K = \frac{2}{3}\frac{\epsilon\mu^3}{\lambda^{3/2}} + O(\epsilon^3) \quad , \tag{3.26}$$

than the energy density at the global minimum. In the case $K \ll \rho$ the effect of this term can be treated as the interaction between the kinks. This is in

the same spirit of the Coleman's thin-wall bubble approximation. (Its effect on the jacobian and the determinants are negligible since we work at the lowest nontrivial order of $\epsilon$.)

Due to the energy density difference, a kink and an antikink have an attractive force between them. The analog lagrangian of this system is given by

$$\mathcal{A}_\epsilon = 2 \int_{-\frac{\beta}{2}}^{\frac{\beta}{2}} d\tau \left( \rho \sqrt{1 + \dot{X}_r(\tau)^2} + K X_r(\tau) \right) \quad , \tag{3.27}$$

where $X_r(\tau)$ denotes the relative coordinate $(Y(\tau) - X(\tau))/2$. Because of the attractive force, the general solutions of this action follow trajectories that are closest at a certain time and go apart from each other to infinite distance asymptotically. (Note that we are looking at the *imaginary-time* solutions.) Their behavior is analogous to the minimum length problem, under a constant force, of a string in 2 dimensional space. The only solution that satisfies the periodic boundary conditions is the trivial one, $X_r(\tau) = 0$. This trivial solution is irrelevant for our purpose, since our background field is only meaningful for separated kinks and antikinks, $X_r(\tau) > 1/\mu$. Intuitively, however, one sees that although an attractive force between kinks and antikinks would reduce their probability of existing with large separation, it would not make the probability of finite separation zero. Therefore we still wish to study the effect of configurations in which the kinks and antikinks have finite separation. In general, in order to evaluate the path-integrals, what we need to do is to take the configurations that have relatively small action and large entropy in the given functional space. This can be carried out by introducing the collective coordinates and using solutions of the kink action, if there are any. When there is none, we can introduce some constraint and look for the minimum solutions under that constraint. After the integrations over the fluctuations within the constraint have been calculated, we can then integrate over the parameter(s) of the constraint to recover the larger functional space.[6]

The choice of the constraint is somewhat arbitrary. It is guided by two considerations. The first is the physical picture of the kinds of the configurations that we wish to include explicitly in this calculation, based on our heuristic picture that kink-antikink effects may be important. The second consideration is more technical — we want to be able to perform the calculation of the contributions of these solutions and fluctuations about them to the path integral. This requires that the introduction of a collective coordinate corresponding to the constrained parameter yields a Jacobian which can be calculated in a similar fashion to that for the collective-coordinate which replaced the zero mode in the previous calculation. The remaining fluctuations must be expanded in a basis where the modes are orthogonal to the change in background field corresponding to a change in the collective coordinate. As we saw above this is trivially true when the background field corresponds to a static kink. Fortunately there is a constraint for which this solution is the *only* periodic solution — we find that is the constraint where the average distance between the kink and antikink is given by $\overline{X}_r$. Appendix B discusses some of the technical details of the imposition of constraints and shows why this choice has the desired features.

The imposition of the constraint is done by the usual Lagrange multiplier method. We require a periodic solution for $X_r(\tau)$ which is an extremum of the quantity,

$$A_\epsilon - \Lambda \int_{-\frac{\beta}{2}}^{\frac{\beta}{2}} d\tau \, (X_r(\tau) - \overline{X}_r) \quad . \tag{3.28}$$

This is given by static solution $X_r(\tau) = \overline{X}_r$. For this solution the fluctuation modes and the Jacobian for the collective coordinate $\overline{X}_r$ are exactly as discussed previously for the case $\epsilon = 0$, which is technically convenient.[7]

Then by analogy to the calculation that led to (3.22) , we find

$$Z_{1,\epsilon}(T) = F_T(\epsilon)\, e^{-2\beta(\rho+\Delta\rho)}\, \frac{\beta\rho}{4\pi}\frac{1}{\beta^2}\int_0^L dY \int_0^Y dX\, e^{-\beta K(Y-X)} \quad ,$$

$$= F_T(\epsilon)\, e^{-2\beta(\rho+\Delta\rho)}\, \frac{\rho}{4\pi\beta}\frac{L}{\beta K}\left(1 - \frac{1}{\beta KL}\left(1 - e^{-\beta KL}\right)\right) \quad . \tag{3.29}$$

The mean probability $\overline{P}$ of being in the unstable phase is given by the following,

$$\overline{P}_{1-bubble}(\epsilon, T) = -\frac{1}{L}\frac{\partial}{\partial(K\beta)} Z_{1,\epsilon}(T) \quad ,$$

$$= F_T(\epsilon) e^{-2\beta(\rho+\Delta\rho)}\, \frac{\rho}{4\pi\beta}\frac{1}{(\beta K)^2}\left(1 - \frac{2}{\beta KL}\right)\left(1 - e^{-\beta KL}\right) \quad . \tag{3.30}$$

Note that in the limit $\epsilon \to 0$, the above result reproduces the previously known result, which contain a factor $1/3$.

First, we sum the contributions of the multi-pairs in the most naive method, the dilute gas approximation treating each *pair* as one object. This is reasonable when the temperature is low enough compared to $K$, so that the attractive force between kink and antikink keeps them close together. This leads to the following,

$$\overline{P}_L(\epsilon, T) = \frac{\sum_{N=1}^{\infty} N\, \overline{P}_{1-bubble}(\epsilon, T)\, \frac{1}{N!}\, Z_{1,\epsilon}(T)^{N-1}}{\sum_{N=0}^{\infty} \frac{1}{N!}\, Z_{1,\epsilon}(T)^N} = \overline{P}_{1-bubble}(\epsilon, T) \,. \tag{3.31}$$

In the limit $L \to \infty$, the above result leads to,

$$\overline{P}_L(\epsilon, T) \to F_T(\epsilon) e^{-2\beta(\rho+\Delta\rho)}\, \frac{\rho}{4\pi\beta}\frac{1}{(\beta K)^2} (\equiv \overline{P}_\infty) \quad . \tag{3.32}$$

This result, however, is not valid for $K\beta \to 0$. Not only that the above result does not reproduce the result derived in the previous subsection, $1/2$, it exceeds the physically acceptable limit, $1/2$, for high enough temperature,

$T > O(\rho/\ln K)$. This is because in evaluating (3.31), we have assumed the tightly bound pairs. When temperature is high enough compared to the attractive force $K$, to overcome the attractive force, the pair spends most of time with large separation. In such a case, the calculation (3.31) overcounts the overlapping tails of the neighboring pairs. In the appendix C, we derive the better expression for $\overline{P}$, doing exactly the summations of the nested integrals of the type (3.29) for finite $L$. In the $L \to \infty$ limit, the result is the following,

$$\overline{P} = \frac{1}{2}\left(1 - \frac{1}{\sqrt{1+4\overline{P}_\infty}}\right) \quad . \tag{3.33}$$

This result is always between 0 and 1/2 and is applicable in all regions of $T < T_c$. This also reproduces (3.31) in the strong binding limit, where $\overline{P}_\infty \ll 1$. The behavior of (3.31) and (3.33) (for $F_T(\epsilon) = 1$) are illustrated in Fig.3. We see that $\overline{P}$ approaches its asymptotic value of 1/2 rather quickly as the temperature becomes high. This behavior is in agreement with the result in the previous subsection. The thermal expectation value $\langle\phi\rangle_T$ is given by (3.23) and (3.33). Its behavior is roughly sketched in Fig. 4.

It should be noted that in (3.29) the integration region included the region $X \cong Y$. This is not exactly correct, because the kink-antikink solution is meaningful only when the kink and antikink are separated by more than their thickness, $1/\mu$. Thus exactly speaking, the integration region for $X$ should be from 0 to $Y - C/\mu$, where C is an appropriate numerical cutoff parameter of order 1. If we do this, $Z_{1,\epsilon}(T)$ is multiplied by a factor $e^{-\beta K \frac{C}{\mu}}$. Our previous result is justified because the effect of this factor is small as long as $K$ is small. Clearly for large $K$ such a term reduces the finite temperature effects of kinks significantly.

# 4. 3+1 DIMENSIONAL CASE

In this section we deal with the case of 3+1 dimensional spacetime. We first investigate the case with the symmetric potential and then briefly mention the case with a energy density difference.

As explained in the section 2, the nonperturbative modes which we wish to include are the bubble-like modes, the excitations of the spherical regions of the other (symmetry-related) vacuum which is surrounded by the domain wall. In order to examine their behavior, we assume the field configuration (background field) to be the following form,

$$\phi_{bubble}(\vec{x},\tau) = \phi_s\left(\frac{|\vec{x}-\vec{X}| - R(\tau,\theta,\varphi)}{\sqrt{1+\dot{R}^2}}\right) \quad , \tag{4.1}$$

where $(\theta,\ \varphi)$ is polar coordinate with the origin $\vec{x} = \vec{X}$. This corresponds to a bubble with a fixed center $\vec{X}$ and a time-dependent radius $R(\tau,\theta,\varphi)$.

For this configuration, the periodic boundary condition is

$$R\left(-\frac{\beta}{2},\theta,\varphi\right) = R\left(\frac{\beta}{2},\theta,\varphi\right) , \quad \frac{\partial}{\partial\tau}R\left(-\frac{\beta}{2},\theta,\varphi\right) = \frac{\partial}{\partial\tau}R\left(\frac{\beta}{2},\theta,\varphi\right) . \tag{4.2}$$

Similarly to (3.18) , the reduced action is,

$$\mathcal{A}_{bubble} = \rho\int_{-\frac{\beta}{2}}^{\frac{\beta}{2}} d\tau \int d\Omega\, R^2\sqrt{1+\dot{R}^2+\frac{1}{R^2}(\vec{L}R)^2} \quad , \tag{4.3}$$

where $\vec{L}$ denotes the angular momentum operator. In deriving (4.3) , we have neglected corrections due to the curvature and acceleration of the bubble. These are negligible provided that $\mu R$ is not small and $\ddot{R}$ is small. As can be seen in (4.3), $\rho$ gives the tension of the boundary wall in this 3+1 dimensional case. The bubble tends to shrink because of this surface tension. This effect leads to

a result similar to that of the previous case where the kink and antikink were attracted to each other due to the energy density difference $\epsilon$. The solutions of the action (4.3) do not obey the periodic boundary condition (except for the trivial and irrelevant solution, $R(\tau) = 0$). Therefore we again need to introduce a constraint. The linear constraint,

$$\frac{1}{4\pi\beta}\int d\tau\, d\Omega R = \overline{R} \quad , \tag{4.4}$$

is the most convenient. The constant solution, $R(\tau,\theta,\varphi) = \overline{R}$, for a given value of $\overline{R}$ is the unique solution for this choice of constraint that satisfies the periodic boundary conditions. (Some of the technical points are given in the second subsection of the Appendix B.) The constant solution allows us to evaluate the relevant quantities as in section 3.3.

The probability of having a single bubble is given by,

$$\Delta_{1b} = \int J_X^3 d\vec{X}\, J_R d\overline{R}\, e^{-4\pi\beta\rho\overline{R}^2} \sqrt{\frac{detD(\phi_{bg}=v)}{det'D(\phi_{bubble})}} \quad . \tag{4.5}$$

The Jacobians $J_X$ and $J_R$ are,

$$J_X = \frac{1}{\sqrt{2\pi}}\sqrt{\int d\tau\; r^2 dr\; d\Omega \left(\frac{\partial\phi}{\partial X_i}\right)^2} = \sqrt{\frac{1}{3}\beta\rho\overline{R}^2} \quad , \tag{4.6}$$

$$J_R = \frac{1}{\sqrt{2\pi}}\sqrt{\int d\tau\; r^2 dr\; d\Omega \left(\frac{\partial\phi}{\partial R}\right)^2} = \sqrt{\beta\rho\overline{R}^2} \quad . \tag{4.7}$$

The ratio of the determinants is evaluated in the appendix A. The result is,

$$\sqrt{\frac{detD(\phi_{bg}=v)}{det'D(\phi_{bubble})}} = F_{T,bubble}\frac{8\sqrt{2}}{\overline{R}^4} \quad , \tag{4.8}$$

where the factor $F_{T,bubble}$ represents the corrections due to the finite population

of the fluctuation modes around the bubble,

$$F_{T,bubble} = \exp\Bigg[-\Bigg(\sum_{l=0}^{c_1\mu\overline{R}}(2l+1)\ln\Big(1-e^{-\beta\sqrt{\frac{l(l+1)+2}{\overline{R}^2}}}\Big)$$

$$+\sum_{l=0}^{c_1\mu\overline{R}}(2l+1)\ln\Big(1-e^{-\beta\sqrt{\frac{l(l+1)}{\overline{R}^2}+\frac{3}{2}\mu^2}}\Big) \qquad (4.9)$$

$$+\sum_{l=0}^{c_1\mu\overline{R}}(2l+1)\int_0^\infty\frac{dk_1}{\pi}\frac{d\delta(k_1)}{dk_1}\ln\Big(1-e^{-\beta\sqrt{\frac{l(l+1)}{\overline{R}^2}+k_1^2+2\mu^2}}\Big)\Bigg)\Bigg] \quad .$$

The cutoff $c_1\mu\overline{R}$ on the sum over angular momenta $l$ occurs because for very high $l$ the approximation of small centrifugal term, which we used to derive the above eigenvalues, breaks down. For high $l$ the eigenvalues in the presence of the bubble and in the absence of the bubble cancel one another. This cancellation is not correctly obtained in our approximation and hence the sum over $l$ in (4.9) must be cut off. A more careful investigation of the comparison of modes with and without the bubble surface shows that our approximation breaks down for $l$ of order $\mu\overline{R}$ and that the contribution of higher modes is negligible on $F_{T,bubble}$. Hence we choose $c_1$ of order 1 in what follows. In the dilute-gas approximation, as used in (3.31), we find,

$$\overline{P}_V = \frac{8\sqrt{2}}{3\sqrt{3}}\beta^2\rho^2\int d\vec{X}\int_{\frac{C}{\mu}}^{\sim V^{1/3}} d\overline{R}\left(\frac{4\pi\overline{R}^3}{3}\right)F_{T,bubble}\,e^{-4\pi\beta\rho\overline{R}^2} \quad , \qquad (4.10)$$

where the lower cutoff $C/\mu$ on the bubble radius is introduced because our approximations on the curvature of the bubble and the thin-walled bubble approximation are invalid when the bubble size becomes of order of the thickness of the bubble wall in (4.1).

For low temperature, $F_{T,bubble} \cong 1$. Therefore in the $V \to \infty$ limit (4.10) leads to,

$$\overline{P}_\infty = \frac{\sqrt{2}}{9\sqrt{3}\pi} G\left(\frac{c_2\mu}{\lambda T}\right) \quad , \tag{4.11}$$

where

$$c_2 \equiv \frac{8\sqrt{2}\pi C^2}{3}, \quad G(x) \equiv (1+x)\, e^{-x} \quad . \tag{4.12}$$

In the region $\lambda T/\mu \ll 1$ where our treatment is valid, the argument of the function G is large and hence we get a exponentially small $\overline{P}$. Thus the thermal expectation value of the field $\phi$, (3.23), is given as follows,

$$\langle\phi\rangle_T = v\left(1 - \frac{2\sqrt{2}}{9\sqrt{3}\pi}\frac{c_2\mu}{\lambda T} e^{-\frac{c_2\mu}{\lambda T}}\right) \quad . \tag{4.13}$$

Therefore, in this temperature range, the effect of the nonperturbative bubbles is exponentially small. This is essentially because the surface tension of the bubbles of the reasonable size $\overline{R} > C/\mu$ costs so much energy that these bubbles are rare in the thermal average at low temperature. Since for small temperature the perturbative correction is of order $\lambda e^{-O(\mu/T)}$, the nonperturbative correction of order $e^{-O(\mu/\lambda T)}$ is really negligible in this region.

For higher temperature, however, $F_{T,bubble}$ is significantly different from zero. Its asymptotic expression is derived in the appendix A. The result is,

$$F_{T,bubble} = e^{A(c_1)\mu^2\overline{R}^2 + O(\mu\overline{R}\ln\mu\overline{R})}, \tag{4.14}$$

where the function $A(c_1)$ is positive definite, and monotonically increasing with $c_1$. For $c_1 \sim 1$, $A(c_1) \sim 4$. Since $F_{T,bubble}$ corrects the integrand in (4.10) by the factor (4.14), it reduces the effective tension for a large bubble. Physically this reduction is actually an entropy effect. The factor $F_{T,bubble}$ grows because of the contribution of low-lying fluctuations in the bubble surface. The number of such

fluctuations which contribute significantly increases with the area of the surface. The effect replaces $\rho$ in (4.10) by

$$\rho \to \rho - \frac{A(c_1)}{4\pi}\mu^2 T \quad . \tag{4.15}$$

Naively interpreted, the expression (4.15) tells us that when the temperature is satisfies

$$T > T_c' = \frac{8\sqrt{2}\pi}{3A(c_1)}\frac{\mu}{\lambda} \quad , \tag{4.16}$$

the tension becomes negative. The $\overline{P}_\infty$ in (4.10) then diverges. As in section 3.3, this divergence signals a breakdown of the dilute-gas approximation. Actually this situation is the same as in the case of (3.32). Once the correlation between the bubbles are taken into account, we would obtain $\overline{P} = 1/2$. In fact at such a temperature, the regions of $\phi(x \in R_\pm) = \pm v$ would be randomly distributed over space. This is quite similar to the order-disorder phase transition in the Ising model. In that model, when the temperature is high enough to overcome the interactions between the adjacent spins, each spin randomly takes either the up or down value. This is understood as the condensate of the domain walls that have become tensionless. The expression (4.15) suggests this picture.

However up till now we have neglected to include in this calculation the effects of order $\lambda T^2$, which we saw in section 2 invalidate the straightforward loop-expansion approach. These effects alone predict a phase transition at a temperature $T_c = 2\mu/\sqrt{\lambda}$, which, for weak coupling, is well below the temperature of order $\mu/\lambda$ where bubble effects become large. For all $T < T_c$, the bubble effects are negligible. A self-consistent treatment, corresponding to the modified loop-expansion discussed in section 2, would replace the quantities $\mu$ and $v$ (and hence $\rho$) in the above equations with their temperature dependent values, $\mu_{\rm eff}(T)$,

$v_{\rm eff}(T)$,

$$\mu^2_{\rm eff}(T) = \mu^2 - \frac{1}{4}\lambda T^2 \,,$$
$$v_{\rm eff}(T) = \sqrt{\frac{\mu^2_{\rm eff}(T)}{\lambda}} \quad , \tag{4.17}$$

This means that the background field at any temperature is chosen as the self-consistent kink solution for the effective action at that temperature, in which the only correction we have is leading term, $\delta S = \frac{1}{4}\lambda T^2\phi^2$. The above procedure is consistent even for the space-dependent configuration. This is true since the single-propagator loop is independent of the external momentum and thus does not give any $\lambda T^2$ correction to the coefficient of the $(\partial\phi/\partial x)^2$ in the expansion of the generating functional. Other graphs can give the finite momentum finite temperature corrections of the form, $\lambda T/m_{\rm eff}(1 + O(k^2/m^2_{\rm eff}))$, where $k$ in an external momentum. Since the kink solution has Fourier components at most of order $k \sim m_{\rm eff}$, these are controlled corrections, which will be included in the determinant of the fluctuations about the kinks. Thus the correction of order $\lambda T^2$ is included in the choice of the background field configuration.[8] The kink solution and kink mass given by $\mu \to \mu(T)$ and $v \to v(T)$ as in (4.17) is a consistent starting point for an estimate of kink effects at finite temperature.[9] When this replacement is made, the kink effects given by (4.10) are tiny at all temperatures below the phase transition temperature at which $\mu^2(T) \to 0$. Right near $\mu^2(T) = 0$, both the modified loop expansion and our nonperturbative thin-walled bubble approximation are unreliable, so we cannot study details of the theory right at the phase transition. In section 5 we will present a physical interpretation of these results.

We have also investigated the case of the Lagrangian (3.25), when there is a energy density difference between two vacua. We find that the constraint on the average radius, (4.4), again allows *only one* periodic solution for a given value of $\overline{R}$. It is the *constant* solution. (This nontrivial result is obtained by using the technique explained in the Appendix B, by drawing the "potential" $-U^2$ for

various values of the parameters $\Lambda$ and $E$. We have exhausted the $\Lambda - E$ plane.) Therefore the calculation for this case is very similar to that presented here. Although we have not fully investigated such theories, one can, for an estimate for small $\epsilon$ case, take the Jacobian and the determinant as the $\epsilon = 0$ value and take into account the $\epsilon$ correction only in the bubble action, as

$$\delta A_{bubble} = \frac{3\pi}{4}\beta\epsilon\overline{R}^3 \quad . \tag{4.18}$$

Then one gets a correction of a factor $1 - O(\epsilon)$ on the rate $\overline{P}$, and the bubble corrections are even less significant in this case, as might be expected. Here we should remark that we are always studying the equilibrium thermodynamics of the system obtained from the true zero temperature vacuum. The case where one assumes that the system is in the false vacuum at some time zero has been studied elsewhere.[10]

## 5. Discussion

We have studied the effects of certain non-perturbative corrections to weak-coupling scalar field theory. In order to intuitively understand the implications of these results we return to the language of Minkowski-space and Hamiltonians used in Section II. For the sake of definiteness let us discuss a lattice version of the theory. The extension of this discussion to a continuum picture is straightforward.

On a lattice we have a scalar field variable $\phi_j$ at each site and a local potential

$$V_j = -\frac{\mu}{2}\phi_j^2 + \lambda\phi_j^4 \tag{5.1}$$

The $(\nabla\cdot\phi)^2$ terms of the Hamiltonian provide couplings between $\phi$ at neighboring sites.

Now consider as a choice of basis states the set of all eigenstates of the potential $V_j$. For states with energies below the barrier ($E < 0$) these will be nearly degenerate pairs of parity even and parity odd $|n\rangle_+$, $|n\rangle_-$ states. These states are <u>not</u> eigenstates of the full Hamiltonian; in fact we know that at zero temperature and infinite volume we have a ground state that has $\langle\phi\rangle = +v$. Hence it is convenient to think in terms of the local superpositions

$$\begin{aligned} |n_j\rangle_R &= |n_i\rangle_+ + |n_i\rangle_- \\ & \qquad\qquad n \ni E_{n_\pm} < 0\,. \\ |n_j\rangle_L &= |n_j\rangle_+ - |n_j\rangle_- \end{aligned} \tag{5.2}$$

(Even though the local states $|n_j\rangle_L$ or $|n_J\rangle_R$ are not orthogonal, the infinite volume states $\prod_j |n_j\rangle_L$ and $\prod_j |n_j\rangle_R$ are.) For states $|n_j\rangle_\pm$ with $E_n > 0$ we have states which lie above the barrier in the local well. The wavefunctions corresponding to these higher states are centered about $\phi_j = 0$. There is no approximation in which it makes sense to think of quasi-stable left and right combinations for these states.

Now the physics of our results can be discussed in the language of these local states. For zero temperature the ground state of the infinite volume system is the state $\prod_j |0_j\rangle_R$ and the low lying excitations are created by the action on this state of some operators

$$\sum_j e^{i\vec{k}\cdot\vec{j}} a^+_{n_j} \tag{5.3}$$

where $a^+_{n_j} |0_j\rangle_R = |n_j\rangle_R$. In this language it is clear that the bubble states which we have included in our calculation correspond to the excitations roughly of the form

$$\prod_{j\in R} |0_j\rangle_L \cdot \prod_{j\notin R} |0_j\rangle_R \ . \tag{5.4}$$

These states are obviously very different from the perturbatively defined low-lying states (5.3).

The calculation of bubble effects with fixed $\mu$ and $v$ takes into account the excitation of regions $R$ which correspond to a dilute gas of spherical bubbles. The low lying excitations about them are treated in harmonic oscillator approximation. This calculation shows an Ising-like order-disorder phase transition at a temperature of order $\mu/\lambda$. The perturbative corrections due to the average interactions between thermally excited modes – the $\lambda T^2$ corrections discussed in Section 2 – become significant at temperatures of order $\mu/\sqrt{\lambda}$. The calculation which ignores these effects is not valid above this temperature. Hence we move to the modified loop expansion, which gives $\mu(T)$ and $\sigma(T)$ in the bubble parameters of Section 4. Then we see that the bubble effects are quite small at all temperatures below the perturbatively calculated phase transition temperature, except in the region $m_{\text{eff}} \to 0$ where both the modified loop-expansion and our thin-walled bubble approximation break down, so we have nothing to say about this region.

In the language of the local states, the phase transition is seen to be due to the increasing probability of exciting finite regions of space into local states which

lie above the barrier and are symmetric about $\phi_j = 0$ rather to the increasing, but still very small, probability of bubble regions of low lying states $\prod_{j\epsilon R} |n_j\rangle_L$. The reason for this is, we believe, an entropy effect. The number of states $|n_j\rangle_\pm$ with $E_n < 0$ is small compared to the number of higher energy states, above the barrier, which are accesible at temperatures of order $\mu/\sqrt{\lambda}$, over finite regions of space.

The conclusions drawn here may be generalized to apply to the potential for the more physically interesting case of a Grand Unified Theory such as $SU(5)$. In general the potential in such a theory has a complicated shape in the space of the various possible vacuum expectation values, with multiple local minima. In the case where there is a $cTr\,\Phi^3$ term in $\mathcal{L}$ (with the $\Phi$ the adjoint representation) there are typically no degenerate gauge distinct minima. Bubbles therefore have volume suppression factors as well as the surface suppression taken into account in our calculation. Hence their contribution at temperatures below the perturbatively calculated critical temperature is even smaller. Thus the argument that the phase transition seen in perturbation theory is driven by the excitation of large regions into states in the part of the well above all structure is therefore stronger here. In fact the entropy factor works further to favor states where the scalar field is symmetric because of the gauge field excitations. These are integrated over to obtain the temperature dependent $V_{\rm eff}$. They tend to favor states with small scalar field expectation values because all gauge fields are massless for zero scalar field expectation values, but some become very massive when there is a symmetry breaking expectation value for any scalar field.[11] This effect is particularly extreme in the case of a Coleman-Weinberg model, where the scalar potential is tuned to be flat at $\langle\Phi\rangle = 0$ at $T = 0$. The local minimum at $\langle\Phi\rangle = 0$ at any finite temperature comes from just such an entropy effect in the gauge field sector.[12]

Unfortunately, this calculation sheds little light on the validity, or otherwise, of the usual approach to early universe cosmology which is based on the study of

the classical evolution of the classical field $\Phi_0$. The probability of supercooling into a metastable state $\langle\Phi\rangle = 0$ for low temperature in a Coleman-Weinberg model is not addressed by this type of calculation. Furthermore the effects of an expanding universe on the nature of the field configurations have not been included here. Mazenko, Unruh and Wald[18] have argued in favor of a bubble-dominated transition because the relative importance of the $(\nabla\Phi)^2$ term in $\mathcal{L}$ is reduced by inflation. It is not within the scope of this calculation to tackle this question.

To summarize our results once again, we have shown that in $1+1$ dimensions, a real scalar field theory undergoes an Ising-like phase transition at zero temperature. For a higher dimensional theory bubble effects are unimportant and the phase transition seen in the modified loop expansion is due to the existance of many local states which are symmetric in $\phi$ rather than to the existance of the degenerate local states in which $\langle\phi(x)\rangle = \pm v$.

# ACKNOWLEDGEMENTS

Helen Quinn would like to acknowledge many conversations with Subhash Gupta, which first stimulated her interest in the interpretation of finite temperature field theory. She also acknowledges conversations with Tom Banks, the comments about gauge theories in section 5 derive much from these conversations. Both authors also acknowledge their colleagues in the SLAC theory group for helpful comments and discussions. This work was supported by the Department of Energy under contract number DE-AC03-76SF00515.

# APPENDIX A

## A.1 1+1 DIMENSION

In this appendix, we evaluate the ratio of determinants for a single kink. For fluctuations around a static kink that satisfies the periodic boundary conditions in $\tau$, the modes are separable in $x$ and $\tau$. The eigenmodes of the $x$-equation consists of the translation zero mode, a bound mode with eigenvalue $\frac{3}{2}\mu^2$, and continuous modes with eigenvalue $k_1^2 + 2\mu^2$. The continuous modes are specified by their phase shift $\delta(k_1)$,

$$\delta(k_1) = -2\arctan\frac{3k\mu}{\sqrt{2}(\mu^2 - k^2)} \quad , \tag{A.1}$$

where branches of the arctan are chosen such that the phase shift is continuous. The boundary values are chosen to be

$$\delta(0) = 2\pi\,, \quad \delta(\infty) = 0\,. \tag{A.2}$$

When restricted to be periodic in a box of length $L$, the eigenvalues of these modes are given by the solutions of the following equation,

$$k_1 + \frac{\delta(k_1)}{L} = k_1^{(0)} \quad , \tag{A.3}$$

where $k_1^{(0)} = \frac{2\pi}{L}m$, ($m$ = integers). For large $L$, this equation can be approximated by,

$$k_1 = k_1^{(0)} - \frac{\delta(k_1^{(0)})}{L} + O\left(\frac{1}{L^2}\right) \quad . \tag{A.4}$$

The $\tau$ direction gives the discreet eigenvalues, $k_0^2$, where,

$$k_0 = \frac{2\pi}{\beta}n\,, \quad (n = \text{integers})\,. \tag{A.5}$$

The ratio of determinants for this one kink configuration can be calculated as

follows,

$$\sqrt{\frac{det D(\phi_{bg}=v)}{det' D(\phi_{one-kink})}} = e^{-I} \quad , \tag{A.6}$$

$$\begin{aligned} 2I =& \sum_n{}' \ln(k_0^2) - \sum_n \ln(k_0^2+2\mu^2) \\ &+ \sum_n \left( \ln(k_0^2+\frac{3}{2}\mu^2) - \ln(k_0^2+2\mu^2) \right) \\ &+ \sum_{n,m} \left( \ln(k_0^2+k_1^2+2\mu^2) - \ln(k_0^2+k_1^{(0)^2}+2\mu^2) \right) \quad . \end{aligned} \tag{A.7}$$

In the above, the prime on the first $\sum$ again means that $k_0 = 0$ mode, which is the constant translation zero mode, should be dropped from the sum. The terms with a minus sign in (A.7) come from the fluctuations about the constant background field. For convenience these subtraction terms have been divided to three parts, the states $k_1 = 0$, the state with $k_1^{(0)} = \frac{2\pi}{L}$ (actually equivalent to $k_1^{(0)} = 0$ in $L \to \infty$), and the rest. This expression shows then the one-to-one correspondence between the modes with and without the kink. The $k_0$-summation is done using the following a $\zeta$-function regularization formula,

$$\sum_{n=1}^{\infty} \ln(a^2n^2+b^2) = -\ln b + \frac{\pi b}{a} + \ln\left(1-e^{-\frac{2\pi b}{a}}\right) \quad . \tag{A.8}$$

Using (A.1) for the $k_1$-terms and doing the partial integral once, we arrive at the following result,

$$I = \ln\beta + \beta\Delta\rho + \ln(1-e^{-\beta\sqrt{\frac{3}{2}}\mu}) + \int_0^{\infty} \frac{dk_1}{\pi} \frac{d\delta(k_1)}{dk_1} \ln(1-e^{-\beta\sqrt{k_1^2+2\mu^2}}) . \tag{A.9}$$

(The first two subtraction terms are cancelled by the boundary value contribution of (A.2).) The first term gives (A.6) the correct dimension, $length^{-1}$ (due to the

absence of one mode that has been replaced by the collective coordinate). The second term correctly reproduces the zero temperature correction to the soliton mass which has been given in literature,

$$\Delta\rho = \left(\frac{1}{2\sqrt{6}} - \frac{3}{\sqrt{2}\pi}\right)\mu \quad . \tag{A.10}$$

(the divergence in (A.7) is already absorbed by the zero temperature renormalization of $\mu$ and not explicitly given here.) The rest of the terms are the usual finite temperature terms due to nonzero population of of the fluctuation modes. ($d\delta/dk_1$ is essentially the difference between the densities of continuous modes with and without the kink.)

## A.2 3+1 DIMENSION

In this appendix we calculate the determinant for a static bubble in 4 dimension using the phase shift given in the 2 dimensional case. One complication in the higher dimensional theory is that the determinant usually contains the Casimir energy term, the energy that depends on the shape and size of the bubble. It, however, is irrelevant in the regions of the parameter space we are interested in, because the surface energy term dominates. Hence we drop their contribution to the determinant.

The eigenvalues of the lower-lying fluctuations are obtained by separating the angular variable, the radius $r$, and the $\tau$. The angular part is given by the usual spherical harmonic functions, $Y_{l,m}(\theta,\varphi)$. We can take the radial function as in the 1-dimensional problem as long as the bubble radius is large and the centrifugal term is small. This is because the centrifugal force term $l(l+1)/r^2$ has a larger contribution at $r = \overline{R}$ than the bubble background field when $l(l+1)/\overline{R}^2 > 1/\mu^2$. In other words, for $l > \mu\overline{R}$, the centrifugal force dominates over the effect of bubble background field. Once the centrifugal term is dominant, the eigenvalues of the fluctuations with and without the bubble are the same. Therefore in the ratio of the determinants, we only need to count $l < c_1\mu R$, with $c_1$ of order 1.

For these $l$, the eigenvalues are given as follows. First, the trapped modes, the modes with the radial part that has the zero radial eigenvalue are obtained by expanding the bubble action (4.3) for $R(\tau,\theta,\varphi)=\overline{R}+\delta R$,

$$A = 4\pi\beta\rho\overline{R}^2 + (linear\ term\ in\ \delta R) + \rho\int d\tau\, d\Omega\left(\delta R^2 + \frac{1}{2}\left(\overline{R}^2\delta\dot{R}^2 + (\vec{L}\delta R)^2\right)\right) \quad . \tag{A.11}$$

Therefore we obtain the eigenvalues of the trapped mode to be

$$\lambda_{k_0,l} = k_0^2 + \frac{1}{\overline{R}^2}(2 + l(l+1)) \quad . \tag{A.12}$$

Among these modes, the $k_0 = 0, l = 0$ mode corresponds to the uniform change of bubble radius, thus the change of the constraint parameter $\overline{R}$. The three $k_0 = 0$, $l = 1$ modes correspond to the uniform spatial translation of the bubble, the change in $\vec{X}$. These modes are dropped from the calculation of the determinants. Note that from the expression (A.12) , none of these modes have zero eigenvalue in contrast to the one-dimensional case. This is because the $l = 1$ mode is the translation mode only infinitesimally. If we have taken a trajectory in the functional space that corresponds to change of the center of the bubble, it has a nonzero (but second order) component to the $l = 0$ direction. Since the action is not extremized in this direction, it is possible not to change the value of the action along this trajectory. In the actual one-loop calculation, however, we simply need to drop these four modes from the determinant.

The other eigenvalues are given by adding the angular term $l(l+1)/\overline{R}^2$ to the one-dimensional values. This is because since within the thin wall approximation we can essentially take a thick spherical shell region $\overline{R} - L < r < \overline{R} + L$ and compare the modes that are confined in that region with and without the bubble. As a result, carrying out the similar calculation to the one in the previous subsection, we obtain the following,

$$\sqrt{\frac{detD(\phi_{bg}=v)}{det'D(\phi_{bubble})}} = \frac{8\sqrt{2}}{\overline{R}^4}F_{T,bubble} \quad , \tag{A.13}$$

where the $1/\overline{R}^4$ term corresponds to the missing eigenvalues, $\sqrt{2}/\overline{R}$ and three of $2/\overline{R}$. The factor $F_{T,bubble}$ is a dimensionless quantity, which is the full ratio of the determinants,

$$F_{T,bubble} = \exp\Bigg[-\Bigg(\sum_{l=0}^{\sim\mu\overline{R}}(2l+1)\ln\Big(1-e^{-\beta\sqrt{\frac{l(l+1)+2}{\overline{R}^2}}}\Big) + \sum_{l=0}^{\sim\mu\overline{R}}(2l+1)\ln\Big(1-e^{-\beta\sqrt{\frac{l(l+1)}{\overline{R}^2}+\frac{3}{2}\mu^2}}\Big) + \sum_{l=0}^{\sim\mu\overline{R}}(2l+1)\int_0^\infty \frac{dk_1}{\pi}\frac{d\delta(k_1)}{dk_1}\ln\Big(1-e^{-\beta\sqrt{\frac{l(l+1)}{\overline{R}^2}k_1^2+2\mu^2}}\Big)\Bigg)\Bigg] \quad . \tag{A.14}$$

(Here we have already dropped the Casimir energy term as was mentioned at the begining of this appendix.)

Let us derive its asymptotic expression for high temperature. First, we expand the exponent in the ln's and take the first two terms.

$$\ln\Big(1-e^{-\beta\sqrt{\frac{l(l+1)}{\overline{R}^2}+\star}}\Big) = \ln\Big(\frac{\beta}{\overline{R}}\Big) + \frac{1}{2}\ln\Big(l(l+1)+\overline{R}^2\star\Big) + \ldots . \tag{A.15}$$

The term proportional to $\ln\beta/\overline{R}$ cancels between the three terms of (A.14). Hence the dominant contribution of the $l$-summation for small $\beta$ and large $\mu\overline{R}$ can be approximated using the following formula,

$$\sum_{l=0}^{X}(2l+1)\ln\Big(l(l+1)+\alpha_2 X^2+\alpha_0\Big) = 2X^2\ln X + \Big((\alpha_2+1)\ln(\alpha_2+1)-\alpha_2\ln\alpha_2-1\Big)X^2 + \mathcal{O}(X\ln X), \tag{A.16}$$

where $X \equiv c_1\mu\overline{R}$. This can be obtained by bounding the upper and lower limits of the sum by continuous integrals and expanding the integrals with respect to

$X$. The first term in the right side of (A.16) again cancels between the three sums of (A.14). Collecting all the coefficients, and carrying out the $k_1$-integration, we find

$$F_{T,bubble} = e^{A(c_1)\mu^2\bar{R}^2 + O(\mu\bar{R}\ln\mu\bar{R})}, \tag{A.17}$$

where the function $A(c_1)$ is,

$$\begin{aligned} A(c_1) = (3+2c_1^2)\ln\left(\frac{\sqrt{4+2c_1^2}+1}{\sqrt{4+2c_1^2}-1}\right) + 2c_1^2\ln\left(\frac{\sqrt{2+c_1^2}+\sqrt{2}}{\sqrt{2+c_1^2}-\sqrt{2}}\right) \\ + 3\sqrt{4+2c_1^2} - 6 - \frac{3}{2}\ln 3\,. \end{aligned} \tag{A.18}$$

This is a positive, monotonically increasing function. For large $c_1$, $A(c_1) \sim 6\sqrt{2}c_1$, and $A(1) = 4.16051928...$ .

# APPENDIX B

In this appendix, we explain some technical details of the analysis of the constraints. The first subsection gives the discussion on the 1+1 dimensional case. The second subsection gives the discussion on the differences of the 3+1 dimensional case from the 1+1 case.

## B.1 1+1 DIMENSION

Let us take a following type of constraint,

$$\int_{-\frac{\beta}{2}}^{\frac{\beta}{2}} d\tau\, F(X(\tau)) = 0 \quad , \tag{B.1}$$

where $F$ is a ordinary function. In order to minimize the action (3.27) under this constraint, we introduce the Lagrange multiplyer $\Lambda$ and extremize the following integral,

$$A_\epsilon - \Lambda \int_{-\frac{\beta}{2}}^{\frac{\beta}{2}} d\tau\, F(X(\tau)) \quad . \tag{B.2}$$

The solution of the above has a constant of "motion", $E$,

$$E = \frac{1}{\sqrt{1+\dot{X}_r^2}} + KX_r - \Lambda' F(X_r) \quad , \tag{B.3}$$

where $\Lambda' \equiv \Lambda/4\pi\rho$. Such a solution is required for a system with the equation of motion,

$$\dot{X}_r^2 - U(X_r)^2 = -1 \quad ,$$

$$U(X_r) = \frac{1}{E - KX_r + \Lambda' F(X_r)} \tag{B.4}$$

Thus the problem is equivalent to the real-time motion of a particle with energy $-1$ in the potential $-U^2$. Note that (B.3) restricts $X_r$ to be in the region $U > 0$.

For a given $F(X_r)$, the behavior of the solutions are easily pictured by drawing $U$ for various values of $E$ and $\Lambda'$. It is straightforward to show that among the constraints of the type $F(X_r) = X_r^n - \overline{X}^n$, only $n = 1$ allows periodic solutions. It can also be seen that the only periodic solution with this constraint is the constant solution, $X(\tau) = \overline{X}$. (This is possible by having the flat "potential", $-U^2 = -1$ by the choice $E = 1$, $\Lambda' = 1$. Since the potential is flat, it is trivial that for these values of the parameters the only periodic solution is the constant one.) In general it is possible to construct more general $F(X_r)$'s that also give a unique periodic solution. However, they would in general require complicated sets of orthonormal modes. Therefore we would not investigate them here. Another possible type of constraint is on the boundary values of $X(\tau)$'s. For example, a possibility is

$$X\left(-\frac{\beta}{2}\right) = X\left(\frac{\beta}{2}\right) = const., \quad \dot{X}\left(-\frac{\beta}{2}\right) = \dot{X}\left(\frac{\beta}{2}\right) = 0 \quad . \tag{B.5}$$

and similarly for $Y$. Although this set of constraints always generates periodic solutions, these solutions are time-dependent and lead to much more complicated calculations, for the Jacobians and the determinant of the fluctuations than the case of a constant solution. Hence we find it convenient to use a constraint of the form (B.1) with $F(X) = X - \overline{X}$.

## B.2 3+1 DIMENSION

As in the previous subsection, we examine the following type of constraints,

$$\int_{-\frac{\beta}{2}}^{\frac{\beta}{2}} d\tau\, F(R(\tau)) = 0 \quad . \tag{B.6}$$

The solutions of this constrained problem satisfy the following equations,

$$\dot{R}^2 - U(R)^2 = -1 \quad , \tag{B.7}$$

$$U(R) = \frac{R^2}{E + \Lambda' F(R)} \quad , \tag{B.8}$$

where $\Lambda' \equiv \Lambda/(4\pi\rho)$. In contrast to the previous case, (B.8) allows various simple constraints that yield periodic solutions. Let us look at the linear constraint, $F = R - \overline{R}$ first. It is straightforward to see that for

$$E = \overline{R}^2, \quad \Lambda' = 2\overline{R} \quad , \tag{B.9}$$

the function $\overline{R}(\tau, \theta, \varphi) = \overline{R}$ solves (B.7). As shown in the Figure 5, this static solution corresponds to the unstable solution of the analog particle problem. It is also easy to see from this figure that for the values of the parameters (B.9) , only the static solution can satisfy the periodic boundary condition, (4.2). Actually for any $E > 0$ and $\Lambda' > 0$, the main features of this "potential" is the same; namely, it has only one extremum, which is a maximum, in the valid region $U > 0$. Thus it is impossible to have a solution that satisfy the periodic boundary condition in this range. By studying other ranges of $E$ and $\Lambda'$, it is also straightforward to see that there is no other periodic solution exists than that given by (B.9).

For some of other types of constraints, the constant solution is no longer unique. For example, let us take a constraint on the average *volume* of the bubble, $F = R^3 - \overline{R}^3$. It is straightforward to see that for negative $\Lambda$, singular or oscillating solutions are possible due to the existance of singularity or minima of the potential. This is essentially because for negative $\Lambda$ the Lagrange-multiplyer term acts as the positive volume energy term. Therefore among the constrained solutions are the bounce solutions used by Linde[10] for discussion of the decay rate of the false vacuum at finite temperature. This type of constraint might still be useful if the constant solution still has the minimum action among the periodic solutions. However we have looked at some of these solutions and have found that this is not the case for our problem. In general, for a given function of $F$ (and a given value of the parameter), there may be many time-dependent solutions that satisfy the periodic boundary condition. These nontrivial time-dependent

solutions usually require evaluations of complicated Jacobians, determinants and the collective coordinate integration. Therefore we conclude that the linear constraint is the most convenient way to characterize bubble configurations.

# APPENDIX C

In this appendix, we give the derivation of (3.33) . In order to do this, we need to deal with the following integrals.

$$I_N(L) \equiv \int_0^L dY_N \int_0^{Y_N} dX_N .... \int_0^{Y_1} dX_1 \, e^{-A(Y_1-X_1)-...-A(Y_N-X_N)} \quad . \tag{C.1}$$

In the actual calculation of $\overline{P}$, $A$ corresponds to $\beta\rho$. For convenience, we can define $I_0(L)$ to be 1. The $I_N$'s then satisfy a reduction formula,

$$\frac{d}{dL}\left(e^{AL}\frac{d}{dL}I_N(L)\right) = e^{AL}\frac{d}{dL}I_{N-1}(L) \quad . \tag{C.2}$$

Now we define

$$f_N(AL) \equiv A^{2N}e^{\frac{1}{2}AL}I_N(L) \quad . \tag{C.3}$$

Then (C.2) leads to,

$$\frac{d^2}{dx^2}f_N(x) - \frac{1}{4}f_N(x) = f_{N-1}(x) \quad . \tag{C.4}$$

If we define the generating functional $W(x,y)$ as follows,

$$W(x,y) \equiv \sum_{N=0}^{\infty} y^N f_N(x) \quad , \tag{C.5}$$

then $W(x,y)$ satisfies the simple differential equation,

$$\frac{d^2}{dx^2}W_(x,y) - \frac{1}{4}W(x,y) = y\,W(x,y) \quad . \tag{C.6}$$

The initial conditions necessary to solve this equation are,

$$W(0,y) = 1\,, \quad \frac{\partial}{\partial x}W(x,y)\Big|_{x=0} = -\frac{1}{2} \quad . \tag{C.7}$$

The solution is

$$W(x,y) = \cosh\left(\frac{1}{2}\sqrt{1+4y}\,x\right) - \frac{\sinh\left(\frac{1}{2}\sqrt{1+4y}\,x\right)}{\sqrt{1+4y}} \qquad (C.8)$$

$$\to \frac{1}{2}\left(1 - \frac{1}{\sqrt{1+4y}}\right) e^{\frac{1}{2}\sqrt{1+4y}\,x} \quad (x \to \infty) \quad .$$

Thus the denominator of (3.31) can be replaced by

$$Z(T) = \sum_{N=0}^{\infty} \alpha^N I_N(L)$$

$$= e^{-\frac{AL}{2}} W\left(AL, \frac{\alpha}{A^2}\right) \qquad (C.9)$$

$$\to \frac{1}{2}\left(1 - \frac{A}{\sqrt{A^2+4\alpha}}\right) e^{\frac{1}{2}\left(\sqrt{A^2+4\alpha}-A\right)L} \quad (x \to \infty) \quad ,$$

where

$$\alpha \equiv F_T(\epsilon) e^{-2\beta(\rho+\Delta\rho)} \frac{\rho}{2\pi\beta} \quad . \qquad (C.10)$$

Therefore $\overline{P}$ is obtained as follows,

$$\overline{P} = -\frac{1}{L}\frac{\partial}{\partial A} \ln Z(T)$$

$$\to \frac{1}{2}\left(1 - \frac{A}{\sqrt{A^2+4\alpha}}\right) \qquad (L \to \infty) \quad . \qquad (C.11)$$

Since the naive calculation in (3.31) corresponds to $\overline{P}_\infty = \alpha/A^2$ in our notation, we obtain (3.33) .

# REFERENCES


1. L. Dolan and R. Jackiw, *Phys. Rev.* **D9** (1974), 3320;
   S. Weinberg, *Phys. Rev.* **D9** (1974), 3357.

2. Appropriate references will be found in;
   H. Umezawa, H. Matsumoto and M. Tachiki, *Thermo Field Dynamics*, (North Holland, New York, 1982);
   A. J. Niemi and G. W. Semenoff, *Annals of Physics* **152** (1984), 105.

3. The treatment of the kinks are, for example, given in;
   R. F. Dashen, B. Hasslacher and A. Neveu, *Phys. Rev.* **D10** (1974), 4114, 4130; R. Rajaraman, *Phys. Rep.* **21** (1975), 227.

4. This factor is mentioned in;
   G. t'Hooft, *Phys.Rev.* **D14** (1976), 3432,
   Errata is in, *Phys.Rev.* **D18** (1978), 2199.

5. A similar result was obtained for the Gross-Neveu model in; R.F.Dashen, S-k.Ma, and R.Rajaraman, *Phys.Rev.* **D11** (1975), 1499.

6. This is in the same spirit of the discussion of the constrained instantons in;
   I. Affleck, *Nucl. Phys.* **B191** (1981), 429.

7. Actually constraints are best treated by the Fadeev-Popov type method. But since the constrained solution turns out to be the same as the symmetric case $\epsilon = 0$, that treatment is not really necessary. We can simply use the previous Jacobian.

8. Notice that this limits our treatment to the region $\mu^2_{\rm eff}(T) > 0$. As $\mu_{\rm eff}(T)$ approaches zero the barrier between the minima at $\pm v(T)$ becomes small and the thin-walled bubble approximation for the kinks becomes invalid. Hence we cannot examine the region near the perturbatively induced phase transition, we can only study the importance of non-perturbative effects in the low temperature region. Of course once $\mu^2_{\rm eff} < 0$ the effective potential has only a single minimum and there are no kink corrections.

9. The source of the shift from $v(0)$ and $\mu(0)$ to $v(T)$ and $\mu(T)$ is the same in the presence of the kink as it was in the constant background field case. It is the effect of the average population of the thermal fluctuations about the background field on the self-consistent choice of background field.

10. A.D.Linde, *Phys.Lett.* **100B** (1981), 37.

11. See also the discussion of entropy effects given by M. Peskin, *Ann.Phys.* **113** (1977), 122.

12. This picture of physics of the Coleman-Weinberg potential at finite temperature was explained to us by Tom Banks.

13. G.N.Mazenko, W.G.Unruh and R.M.Wald, preprint: *Does a Phase Transition in the Early Universe Produce the Conditions Needed for Inflation?*

# FIGURE CAPTIONS

1. The mass insertion diagram described in the text as the single-propagator loop graph.

2. Behaviors of the thermal expectation value of the field operator $\langle\phi\rangle_T$. The physical solution is indicated by a dashed line, and the unphysical solution which corresponds to a negative value for the square of the physical mass is indicated by a dash-and-dot line.

3. The fraction of space $\overline{P}$ in which the expectation value of $\phi(x)$ is in the unstable minimum is shown as a function of temperature. The physical quantity $\overline{P}$ given by (3.33) is shown by the solid lines. The unphysical naive estimate $\overline{P}_\infty$ is shown by the dashed lines. The parameter $\gamma$ is defined by $\gamma \equiv \dfrac{K}{\rho} = \dfrac{4\epsilon\sqrt{\lambda}}{3\mu^3}$. For the ease of calculation, we took here $F_T(\epsilon) = 1$.

4. The nonperturbative effects on the thermal expectation value $\langle\phi\rangle_T$ for the 1+1 dimensional symmetric case is illustrated for (a) the symmetric case and (b) the nonsymmetric case ($\epsilon \neq 0$) for very small $\epsilon$. The dashed lines represent the perturbative value $v(T)$. The solid lines give the value including the nonperturbative effect. Since the high temperature behavior of this theory is not known, only the low temperature part is illustrated.

5. The "potential" $-U^2$ is illustrated for the values of the parameters (B.9). The fat arrow shows the allowed region $U > 0$.

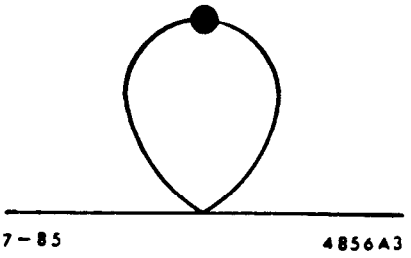


Fig. 1

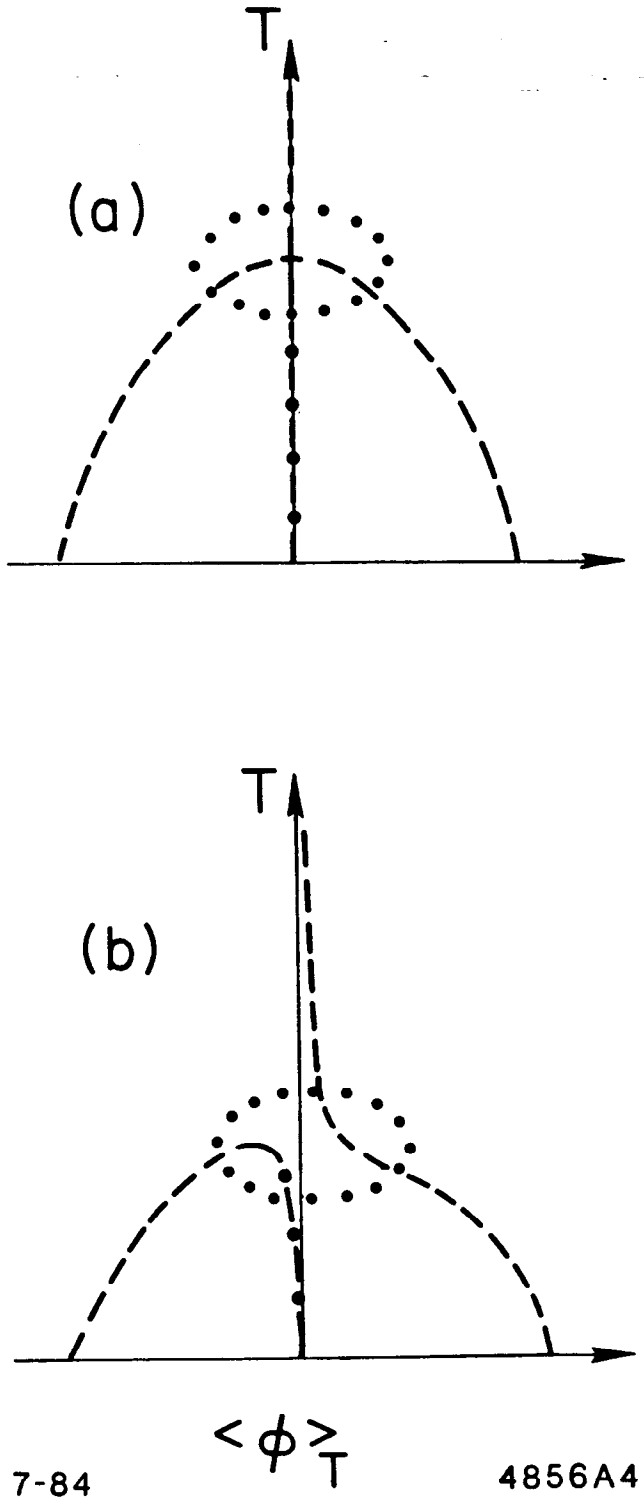


Fig. 2

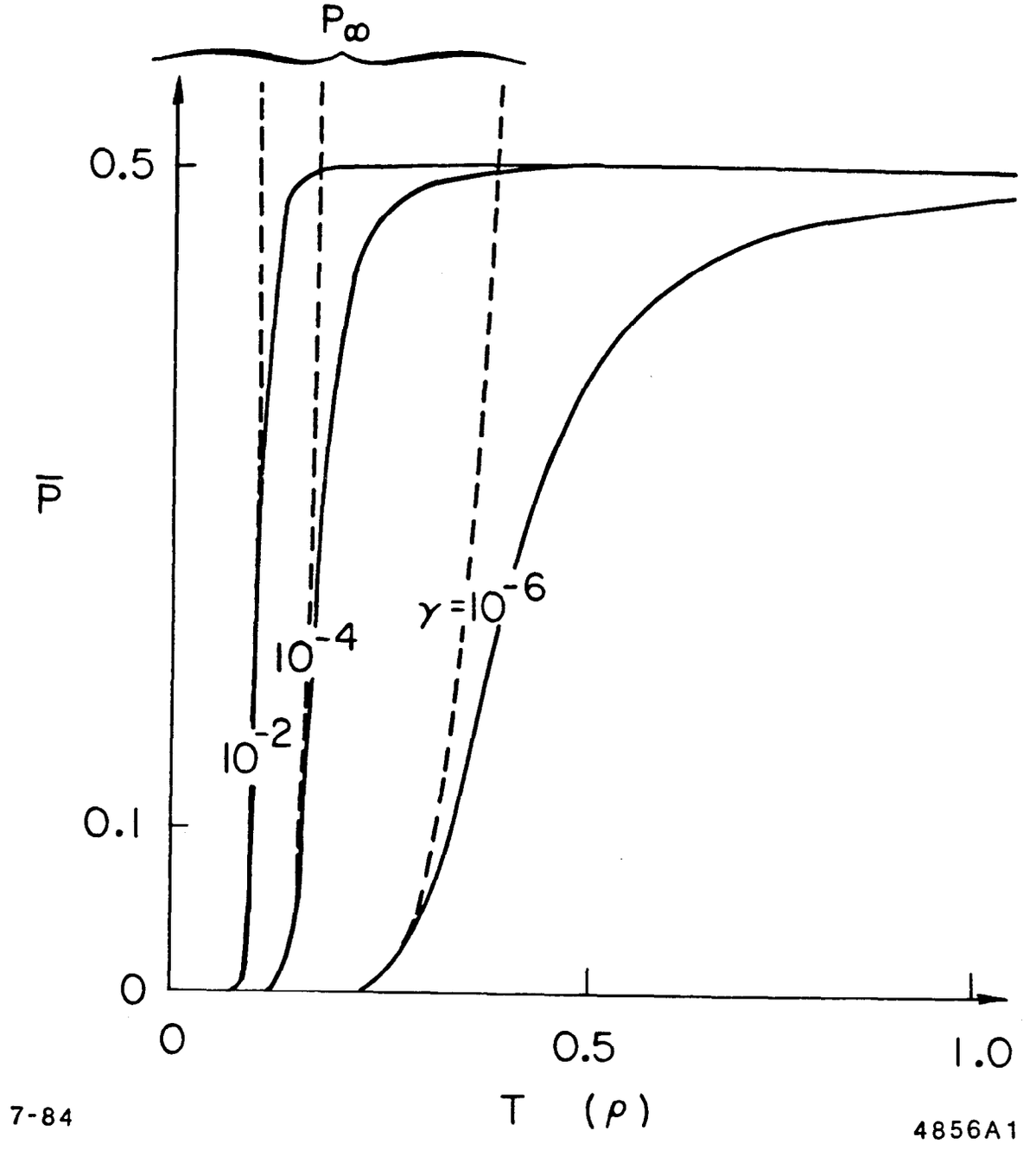


Fig. 3

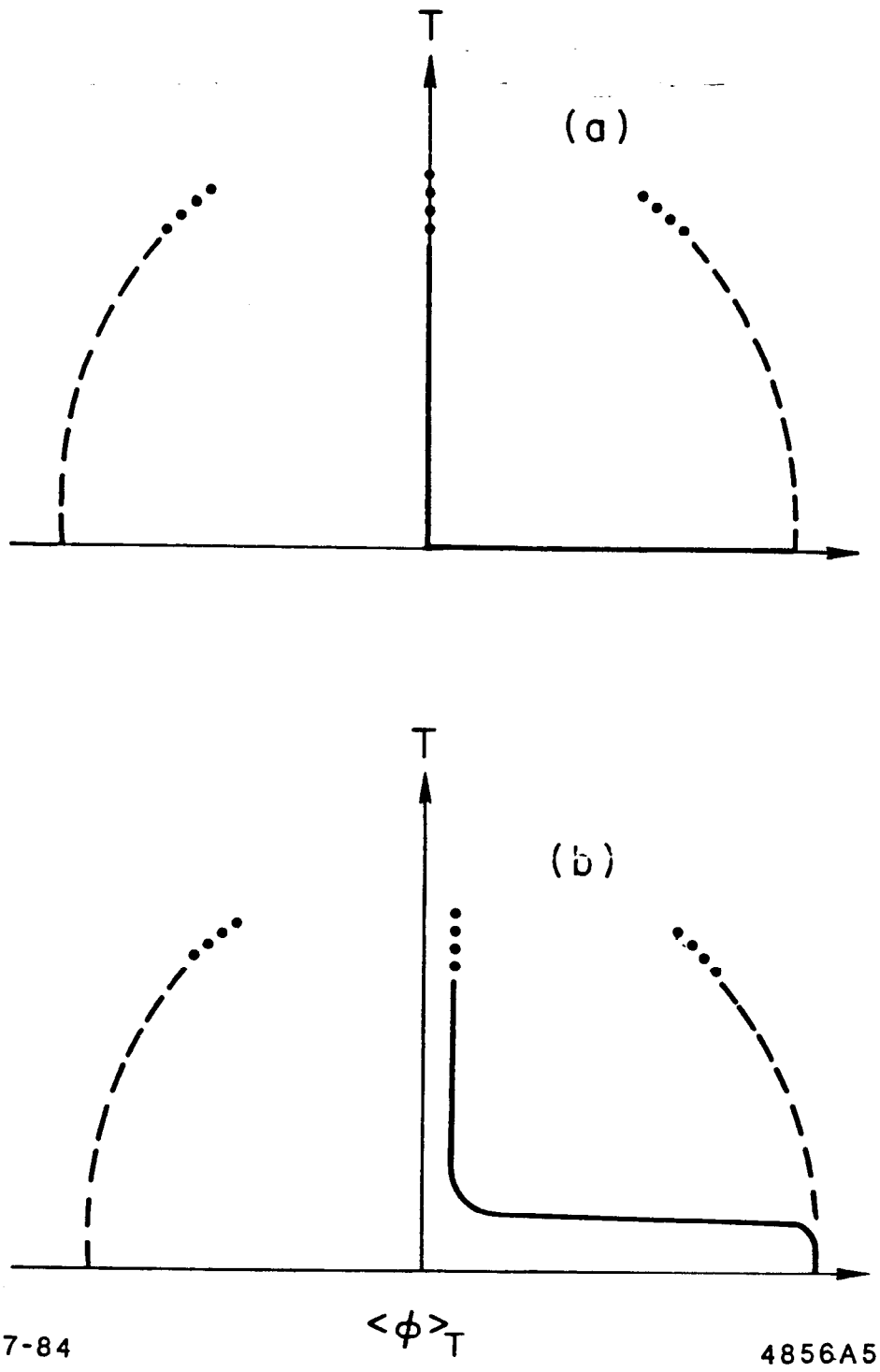


**Fig. 4**

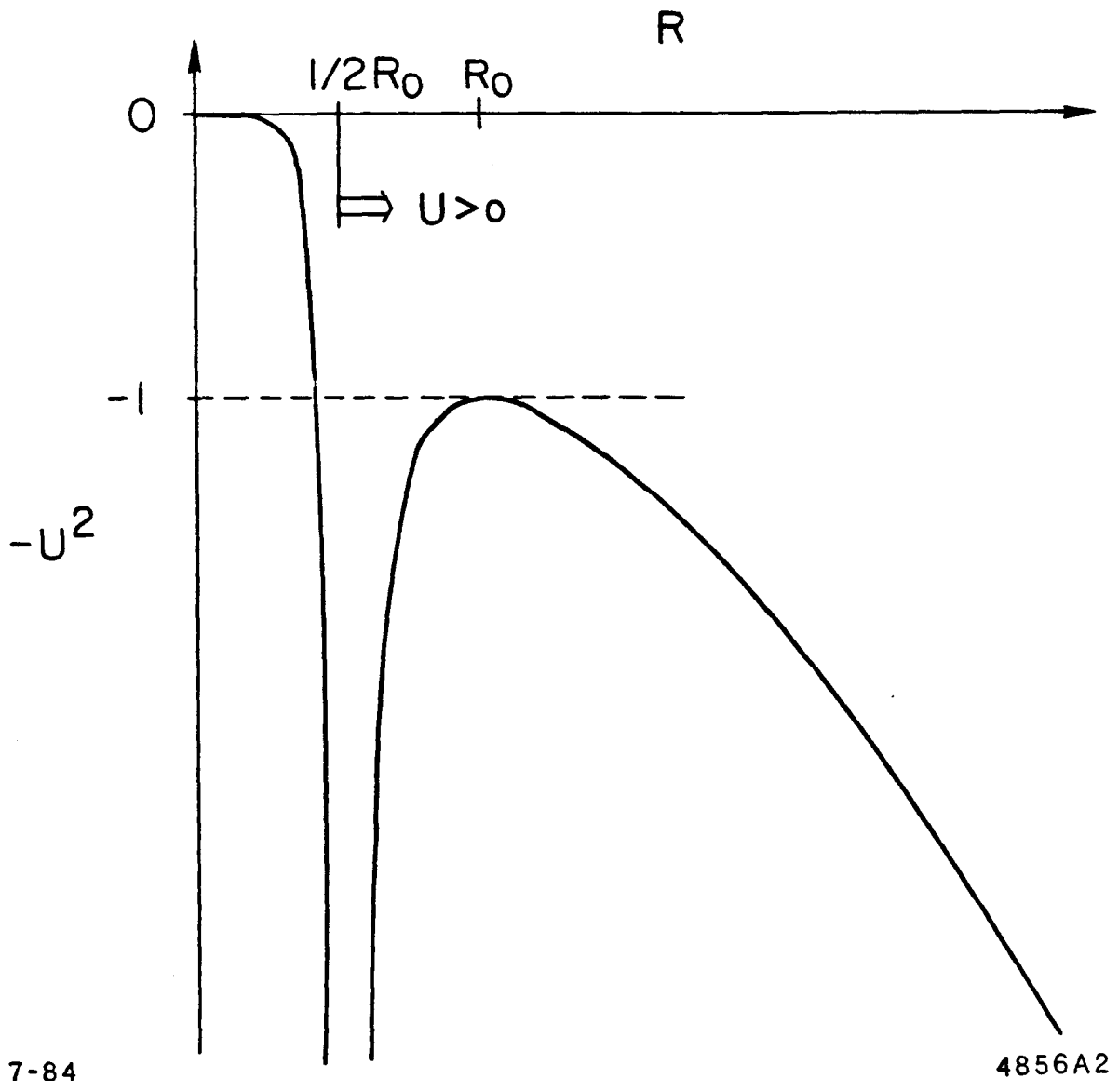


Fig. 5